

Journal of Visualized Experiments

Advanced imaging of lung homing human lymphocytes in an experimental in vivo model of allergic inflammation based on light-sheet microscopy

--Manuscript Draft--

Article Type:	Invited Methods Collection - JoVE Produced Video
Manuscript Number:	JoVE59043R1
Full Title:	Advanced imaging of lung homing human lymphocytes in an experimental in vivo model of allergic inflammation based on light-sheet microscopy
Keywords:	lung homing, peripheral blood mononuclear cells, light-sheet fluorescence microscopy, allergic lung inflammation, three dimensional imaging
Corresponding Author:	Anja Schulz-Kuhnt GERMANY
Corresponding Author's Institution:	
Corresponding Author E-Mail:	Anja.Schulz-Kuhnt@uk-erlangen.de
Order of Authors:	Anja Schulz-Kuhnt Sebastian Zundler Anika Grüneboom Clemens Neufert Stefan Wirtz Markus F. Neurath Imke Atreya
Additional Information:	
Question	Response
Please indicate whether this article will be Standard Access or Open Access.	Standard Access (US\$2,400)
Please indicate the city, state/province, and country where this article will be filmed . Please do not use abbreviations.	Erlangen, Bavaria, Germany

To
Dr Payel Sil
Guest Editor
JoVE

12.12.2018

Dear Dr Sil,

We are pleased to submit a revised version of our manuscript **JoVE59043** for potential publication in the scheduled JoVE Methods Collection "Comprehensive Guide to Inflammation Detection Methodologies". To address all editorial and Reviewers' comments adequately, we now carefully revised our manuscript, extended the Discussion, included a new subfigure into Figure 1 and made some additional clarifications. Based on a comment provided by Reviewer #2, we changed the title of our manuscript; it is now entitled "Advanced imaging of lung homing human lymphocytes in an experimental *in vivo* model of allergic inflammation based on light-sheet fluorescence microscopy". All text passages, which have been added or modified in response to the Reviewers' comments, are indicated (underlined text).

Moreover, we performed some additional experimental analyses in order to address the fifth comment of Reviewer #1. These data have been included into our Point-by-Point reply. We believe that the revision process markedly strengthened the manuscript and hope that the revised paper will meet the requirements for publication in JoVE.

We are looking forward to hearing from you.

Sincerely yours,

Imke Atreya, MD PhD
Department of Medicine 1, University Hospital of Erlangen

TITLE:

Advanced imaging of lung homing human lymphocytes in an experimental in vivo model of allergic inflammation based on light-sheet microscopy

AUTHORS:

Anja Schulz-Kuhnt¹, Sebastian Zundler¹, Anika Grüneboom², Clemens Neufert¹, Stefan Wirtz¹, Markus F. Neurath¹, Imke Atreya¹

¹ Department of Medicine 1, University Hospital of Erlangen, Erlangen, Germany

² Department of Medicine 3, University Hospital of Erlangen, Erlangen, Germany

Corresponding Author:

Imke Atreya

Imke.Atreya@uk-erlangen.de

Email Addresses of Co-authors:

Anja Schulz-Kuhnt (Anja.Schulz-Kuhnt@uk-erlangen.de)

Sebastian Zundler (Sebastian.Zundler@uk-erlangen.de)

Anika Grüneboom (Anika.Klingberg@uk-erlangen.de)

Clemens Neufert (Clemens.Neufert@uk-erlangen.de)

Stefan Wirtz (Stefan.Wirtz@uk-erlangen.de)

Markus F. Neurath (Markus.Neurath@uk-erlangen.de)

KEYWORDS:

lung homing, peripheral blood mononuclear cells, light-sheet fluorescence microscopy, allergic lung inflammation, three-dimensional imaging

SUMMARY:

The here introduced protocol allows characterization of the lung homing capacity of primary human lymphocytes under in vivo inflammatory conditions. Pulmonary infiltration of adoptively transferred human immune cells in a mouse model of allergic inflammation can be imaged and quantified by light-sheet fluorescence microscopy of chemically cleared lung tissue.

ABSTRACT:

Overwhelming tissue accumulation of highly activated immune cells represents a hallmark of various chronic inflammatory diseases and emerged as an attractive therapeutic target in the clinical management of affected patients. In order to further optimize strategies aiming at therapeutic regulation of pathologically imbalanced tissue infiltration of pro-inflammatory immune cells, it will be of particular importance to achieve improved insights into disease- and organ-specific homing properties of peripheral lymphocytes. The here described experimental protocol allows to monitor lung accumulation of fluorescently labeled and adoptively transferred human lymphocytes in the context of papain-induced pulmonary inflammation. In contrast to standard in vitro assays frequently used for the analysis of immune cell migration and chemotaxis, the now introduced in vivo setting takes into account lung-specific aspects of

tissue organization and the influence of the complex inflammatory scenario taking place in the living murine organism. Moreover, three-dimensional cross-sectional light-sheet fluorescence microscopic imaging does not only provide quantitative data on infiltrating immune cells, but also depicts the pattern of immune cell localization within the inflamed lung. Overall, we are able to introduce an innovative technique of high value for immunological research in the field of chronic inflammatory lung diseases, which can be easily applied by following the provided step-by-step protocol.

INTRODUCTION:

Classic inflammatory disorders of the lung, such as allergic asthma and chronic obstructive pulmonary disease (COPD), are well known to be driven by an increased recruitment of activated lymphocytes into the pulmonary tissue^{1,2}. Lymphocyte-released cytokines (e.g., IL-4, IL-5, IL-9, IL-13, IFN- γ and TNF- α) further promote chemotaxis of innate and adaptive immune cells, induce fibrotic airway remodeling or directly damage the lung parenchyma². So far, the underlying mechanisms responsible for the pathological accumulation of lymphocytes within lung tissue are not yet fully understood. In analogy to tissue-selective T cell imprinting described for gut and skin homing, pulmonary dendritic cells (DCs) are obviously able to prime peripheral T cells for preferential lung infiltration, at least partly via the induction of CCR4 expression on the surface of lymphocytes³. Besides CCR4, airway-infiltrating T cells are also characterized by a particularly increased expression of the chemokine receptors CCR5 and CXCR3 compared to T cells within the peripheral blood^{1,4,5}. Overall, existing data are consistent with the concept that lung homing of T lymphocytes under physiological or inflammatory conditions involves a number of different chemokine receptors and their respective ligands and thus crucially depends on a closely controlled collaboration between innate and adaptive immune cells¹. Especially, during the initial phase of pathogen or allergen exposure, cells of the innate immune system respond to TLR stimulation or to IgE-mediated cross-linking by the immediate release of different chemoattractants, like LTB₄, CCL1, CCL17, CCL22, CCL20, CXCL10 and PGD₂^{1,6,7}. As a prime example, the interaction between PGD₂ and the chemoattractant receptor CRTh2 is known to be of particular importance for chemotaxis of Th2 cells and thus appeared as promising therapeutic target in the clinical management of asthma. Indeed, patients with moderate asthma showed an improvement of symptoms and a significant increase of the forced expiratory volume in one second (FEV₁) after treatment with a selective CRTh2 antagonist compared to the placebo group^{8,9}. In a more progressed state of the inflammatory response, already recruited T cells are able to further amplify pulmonary lymphocyte accumulation via the release of IL-4 and IL-13 as potent stimuli for pulmonary DCs. Subsequently, these myeloid-derived innate cells up-regulate the expression of CCL17 and CCL22 in a STAT6-dependent manner^{1,10,11}. Although the complexity of the described scenario still hinders a complete understanding of T cell lung homing, it offers a plethora of molecular targets for a potentially optimized therapeutic control of inflammatory or allergic pulmonary diseases. Therefore, there is an urgent need of innovative experimental techniques, which are able to further deepen and complement our knowledge in the field of T cell chemotaxis and lung homing.

Due to the fact that lung homing of lymphocytes within the human body is influenced by

multiple cellular, humoral and physical parameters¹, most of the existing experimental methods are not able to model the whole complexity of this immunological process. Instead, many standard protocols for the analysis of lung homing selectively focus on a specific aspect involved in the cascade of lymphocyte attraction, adhesion, migration and retention. Besides a purely descriptive determination of the mRNA or protein expression pattern of integrins and chemokine receptors on peripheral or lung-infiltrating lymphocytes and the complementary measurement of respective chemokine levels in blood, bronchoalveolar lavage (BAL) or pulmonary tissue¹²⁻¹⁵, well-established in vitro cell culture assays allow a functional characterization of lymphocyte adhesion or chemotaxis upon defined experimental conditions¹⁶⁻¹⁸. In principle, static in vitro adhesion assays monitor the binding capacity of cultured lymphocytes to an endothelial monolayer or to glass slides coated with recombinant endothelial adhesion molecules (e.g., MAdCAM-1, VCAM-1), while standard in vitro chemotaxis assays are usually applied in order to quantify the ability of lymphocytes to migrate along a chemokine gradient in a Transwell system¹⁹. Both in vitro settings enable a controlled adjustment and modulation of experimental conditions, but on the other hand lack important variables known to critically impact on in vivo chemotaxis and adhesion of lymphocytes. Predominantly, static cell culture assays disregard the influence of shear forces caused by the permanent blood flow¹⁹ and potentially neglect the involvement of the surrounding immunological milieu and interacting non-lymphocyte immune cells, both present in a living organism. In order to overcome these limitations, the interpretation of results acquired in static in vitro chemotaxis or adherence assays need further validation in dynamic adhesion experiments under flow conditions^{20,21} and in in vivo models of inflammatory organ pathology¹⁹. Indeed, important conclusions on the regulation of T cell lung homing under inflammatory or allergic conditions could be drawn from animal studies analyzing genetically modified mice in defined models of different pulmonary diseases^{3,22,23}. The quantitative comparison of lung infiltrating lymphocytes between wildtype mice and mice with a deficiency for a specific gene of interest represents a well-established and broadly used tool for defining the impact of particular cellular pathways or receptors on the disease-driven pattern of T cell distribution. However, in contrast to before discussed in vitro cell culture assays, a study design based on classical animal models lacks the ability to analyze and monitor primary human T cells directly derived from the blood or BAL of patients suffering from an inflammatory lung disease. Thus, it still remains challenging to functionally validate whether a diagnostically specified lung disease is able to imprint human lymphocytes for preferential lung tropism and how far clinical parameters might impact on this scenario. Recently, a very elegant in vivo approach was introduced in the context of inflammatory bowel diseases (IBD), which was able to overcome most of these limitations and opened new avenues for advanced translational studies on intestinal lymphocyte homing²⁴. Taking advantage of protocols for solvent-based tissue clearing followed by cross-sectional light-sheet fluorescence microscopy as a powerful imaging tool, it was possible to visualize the infiltration and distribution of adoptively transferred human T cells in the intestine of colitic immunodeficient mice²⁴. In particular, this experimental setting implemented two main innovations: (1) Primary human immune cells can be analyzed under experimentally defined in vivo conditions; (2) a rather large area of the diseased organ (about 1.5 cm x 1.5 cm) can be imaged in high resolution quality, followed by 3D-reconstruction. Moreover, several recent studies successfully established the use of solvent-based tissue

clearing and light-sheet fluorescence microscopy as important tools for advanced lung imaging^{25,26}. In order to benefit from this technological progress in the field of pulmonary immunology, we now adopted the system for analysis of lung homing.

The here presented protocol provides a step-by-step introduction how to purify and fluorescently label primary human T cells for transfer into mice with induced pulmonary inflammation and, moreover, describes in detail the subsequent process of light-sheet fluorescence microscopic imaging, including organ preparation and image processing. Overall, we hope to support future translational studies in the field of inflammatory or allergic lung diseases by introducing a sophisticated, but nevertheless feasible, experimental model for monitoring human lymphocyte lung homing upon in vivo conditions.

PROTOCOL:

Experiments involving animals were performed in accordance with protocols approved by the relevant local authorities in Erlangen (Regierung von Unterfranken, Würzburg, Germany). Mice were housed under specific pathogen-free conditions. The collection of human blood was approved by the local ethical committee and the institutional review board of the University of Erlangen-Nuremberg. Each patient gave written informed consent.

1. Induce allergic lung inflammation in mice

NOTE: As described in earlier studies²⁷, the following experimental procedure allows inducing allergic airway inflammation in mice and, accordingly, triggers the accumulation of innate and adaptive immune cells in the BAL. The described protocol has been established in C57BL/6J mice, but adoption to other standard inbred strains should be possible.

See **Figure 1A** for a summary of the in vivo experimental procedure.

1.1. Anesthetize mice by intraperitoneal injection of ketamine/xylazine.

NOTE: Only use C57BL/6J mice older than 6 weeks and with a body weight of at least 16 g.

1.1.1. Prepare ketamine/xylazine solution in PBS (12 mg/mL ketamine; 1.6 mg/mL xylazine) and determine the exact body weight of mice.

1.1.2. Inject the first mouse with 8 μ L/g bodyweight of ketamine/xylazine solution intraperitoneally and confirm deep anesthesia via the absence of the paw pinch reflex before proceeding to step 1.3.

1.2. Freshly prepare 5 mg/mL of papain in PBS. Slowly pipette 10 μ L (50 μ g) of the papain solution into the nostril. Carefully monitor the mouse until awakening.

1.3. Repeat steps 1.1 and 1.2 for all mice included in the experiment. Perform steps 1.1 – 1.3

on three consecutive days.

2. Purify and fluorescently label human peripheral blood CD4⁺ T cells

NOTE: Process cells under sterile conditions.

2.1. Collect 18 mL of full human blood from a peripheral vein. Perform Ficoll-Hypaque gradient centrifugation in order to select the fraction of peripheral blood mononuclear cells (PBMC).

NOTE: Collection and analysis of primary human material need to be approved by the local ethical authorities. Only a person with an adequate medical qualification is allowed to collect blood from a peripheral vein.

2.1.1. Collect blood in ethylenediaminetetraacetic acid (EDTA)-containing monovettes (1.6 mg EDTA/mL blood) in order to avoid coagulation.

OPTIONAL: Use buffy coat blood, a by-product of blood donation enriched in leukocytes, instead of complete venous blood.

2.1.2. Transfer blood into a conical 50 mL-tube and dilute 1:2 in phosphate buffered saline (PBS). Carefully add 12 mL of Ficoll-medium (density 1.077 g/mL) as a bottom layer under the diluted blood. Centrifuge the sample ($800 \times g$ for 15 min at room temperature without brake).

2.1.3. Carefully remove the tube from the centrifuge and transfer the PBMC-containing interphase into a new conical 50 mL-tube. Discard the upper and bottom layer. Fill the PBMC-containing tube with PBS and centrifuge ($300 \times g$ for 10 min at 4 °C). Remove the supernatant.

NOTE: Optionally, if necessary, perform lysis of remaining erythrocytes. Carefully add 3 mL of ammonium-chloride-potassium (ACP) lysis buffer (155 mM ammonium chloride; 19 mM potassium hydrogen carbonate and 0.68 mM EDTA; pH 7.27) to the resuspended cell pellet and vortex the sample. Shake the tubes for 3 min. To remove the ACP lysis buffer, add 40 mL of PBS and centrifuge ($300 \times g$ for 10 min at 4 °C). Discard supernatant.

2.2. Purify CD4⁺ T cells via CD4 microbeads.

NOTE: In general, there are several distributors of magnetic microbeads for purification of human CD4⁺ cells, which should result in comparable levels of cell purity. Product choice should be based on individual preferences. The following steps of the protocol (2.2.2 - 2.2.7) are adjusted to a defined CD4 microbead product and respective separation columns as further indicated in the **Table of Materials**. Some modifications of the protocol might be required in case that an alternative CD4 microbead product is selected.

2.2.1. Resuspend the PBMC pellet in a minimum of 80 µL PBS containing 0.5% fetal bovine

serum (FBS) and 2 mM EDTA (PBS/FBS/EDTA-buffer) per 10^7 PBMC. Use a starting population of about 30×10^6 PBMC in order to end-up with approximately 3×10^6 to 6×10^6 purified human $CD4^+$ T cells.

2.2.2. Add 20 μ L of $CD4$ microbeads per 10^7 PBMC, mix gently and incubate for 20 min at 4 °C. Fill the tube with PBS/FBS/EDTA-buffer (cooled down to 4 °C) and centrifuge ($300 \times g$ for 10 min at 4 °C). Remove supernatant.

2.2.3. Place a separation column into a magnetic field. Rinse the column with 3 mL of PBS/FBS/EDTA-buffer. Resuspend the cell pellet in 500 μ L of PBS/FBS/EDTA-buffer (cooled down to 4 °C) and transfer the cell suspension onto the rinsed separation column placed within a magnetic field.

2.2.4. Rinse the separation column three times with 3 mL of PBS/FBS/EDTA-buffer (cooled down to 4 °C) and discard the effluent.

2.2.5. Remove the separation column from the magnetic field and place it into a 15 mL-tube. Elute the $CD4^+$ cell fraction in 5 mL of PBS/FBS/EDTA-buffer by using the plunger.

2.2.6. Fill the tube with PBS and centrifuge ($300 \times g$ for 10 min at 4 °C). Remove supernatant. Repeat this washing step twice.

2.2.7. Determine the number of yielded cells by a standard method of choice (e.g., Neubauer chamber).

2.3. Label $CD4^+$ T cells with a fluorescent cell proliferation dye.

2.3.1. Resuspend $CD4^+$ T cells in PBS (up to 10^7 cells/mL; do not use less than 500 μ L of PBS).

2.3.2. Prepare a 6 μ M solution of a red light-excitable cell proliferation dye (see **Table of Materials**) in PBS (pre-warmed to room temperature). Mix this solution 1:2 with the before prepared cell suspension and vortex thoroughly (3 μ M final concentration).

2.3.3. Incubate for 10 min at 37 °C (protected from light). Afterwards, add five volumes of RPMI medium containing 10% FBS and incubate for 5 min on ice (protected from light).

2.3.4. Wash labeled cells three times in RPMI medium containing 10% FBS (centrifuge at $300 \times g$ for 10 min at 4 °C). Resuspend labeled cells in PBS, store on ice and protect from light until use.

NOTE: Prolonged storage of cells (>60 min) might negatively impact on cell survival.

OPTIONAL: Determine the purity of the $CD4^+$ cell fraction and the efficacy of the labeling procedure by flow cytometry. Resuspend 0.5×10^6 to 1×10^6 $CD4^+$ cells in 100 μ L of buffer (1%

FBS, 2 mM EDTA in PBS) and add an anti-human CD4 antibody coupled with a fluorescent dye of choice. Incubate for 30 min at 4 °C. Add 1 mL buffer and centrifuge ($300 \times g$ for 10 min at 4 °C). Discard supernatant. Proceed with flow cytometric measurement of the sample (representative result is depicted in **Figure 1B,C**).

3. Adoptively transfer human CD4⁺ T cells into papain-exposed recipient mice

NOTE: See **Figure 1A** for a summary of the in vivo performed experimental procedure. Perform cell transfer one day after the last intranasal administration of papain.

3.1. Adjust the suspension of fluorescently labeled human CD4⁺ T cells (step 2.3.4) to a concentration of 1×10^7 cells/mL in PBS. Fill 100 μ L of the cell suspension into a 1 mL/30 G-syringe.

3.2. Carefully place the first papain-exposed C57BL/6J mouse (steps 1.1 – 1.3) into a restraint device for tail vein injection. Use the prepared syringe (step 3.1) to puncture the tail vein and slowly inject 100 μ L of the cell suspension containing 1×10^6 labeled human CD4⁺ cells. Do not immediately pull out the needle after injection, but wait for additional 5 seconds in order to prevent discharge of the cell suspension.

3.3. Release the mouse from the restraint device and proceed with the next animal. Keep at least one papain-exposed animal, which does not undergo transfer with fluorescently labeled cells to serve as negative control for light-sheet fluorescence microscopy.

4. Prepare lung tissue for light-sheet microscopy

NOTE: The following steps are performed 3 h after transfer of fluorescently labeled human cells (step 3.2). The described experimental procedures including harvesting of lung tissue, fixation and solvent-based tissue clearing were adapted from currently described protocols^{24,28}.

4.1. Sacrifice the mouse by carbon dioxide (CO₂) inhalation.

4.2. Perfuse the lung in situ with PBS containing 5 mM EDTA.

4.2.1. Open the thorax via cutting along the sternum to expose the heart. Punctate the right ventricle with a 21 G cannula connected to a catheter.

4.2.2. Open the left ventricle by cutting and thereby allow the blood and perfusion fluid to exit. Slowly perfuse the lung with 20 mL of ice-cold PBS containing 5 mM EDTA via the catheter.

4.3. In order to perform in situ fixation of the lung, do not remove the catheter from the right ventricle. Slowly perfuse the lung with 2 mL of ice-cold 4% paraformaldehyde (PFA) solved in PBS. Remove the catheter and the cannula.

NOTE: PFA-based in situ fixation of lung tissue represents a well-established technique in order to prepare murine lung tissue for subsequent microscopic analysis^{29,30}.

CAUTION: PFA is toxic and has to be handled under a hood with care.

4.4. Fill the lung with 0.75% agarose in situ.

4.4.1. Prepare 0.75% agarose in PBS and keep it solid at 50 °C in a thermo-shaker until use. Remove the salivary glands of the mouse, cut the sternohyoid muscle and expose the trachea by sliding a forceps underneath.

4.4.2. Punctuate the exposed trachea with a 30 G needle and replace it by a blunt 30 G catheter to prevent further damage of the trachea resulting in undesired leakage of agarose. Seal the junction between the inserted catheter and the trachea.

OPTIONAL: Combine the here described procedure with BAL collection to analyze infiltrated human cells in BAL as recently described in detail³¹ (see **Figure 2E** for representative results).

4.4.3. Carefully fill the airways with 0.75% agarose (cooled down to body temperature) via the catheter until complete unfolding of the lung; wait until complete solidification of the agarose. Remove the catheter and carefully harvest the lung in a darkened 2 mL-tube filled with 4% PFA.

4.5. For additional fixation incubate the sample in 4% PFA solved in PBS for 2 h at 4 °C under continuous rotation (31 rpm).

4.6. Dehydrate tissue by subsequently incubating the sample under continuous rotation (31 rpm) at 4 °C in 50% ethanol (pH 9), 70% ethanol (pH 9) and 100% ethanol; each step for at least 4 h. At the end, perform a second incubation in fresh 100% ethanol for 4 h.

4.7. Perform solvent-based clearing of the tissue using ethyl cinnamate (ECi). Therefore, transfer the sample into ECi. Incubate overnight at room temperature (under constant rotation) until the tissue appears translucent (see Figure 1D for representative images).

NOTE: Samples stored in ECi at room temperature (protected from light) are stable over several weeks to months.

5. Perform light-sheet fluorescence microscopy of whole murine lung lobes

NOTE: Please see the **Table of Materials** for details on the light-sheet fluorescence microscope and the corresponding software, on which the following steps are based. Comparable systems by other manufacturers, however, can be used as well with developer-specific modifications of the following protocol. Before starting, get familiar with the microscope-specific operating manual and follow the technical instructions by the responsible person on site.

5.1. Set up the light-sheet microscope.

5.1.1. Turn on the light-sheet microscope and open the corresponding imaging software on the computer. Fill the sample chamber with filtered ECI (100 μm filter) and place it in its position between the laser beams.

5.1.2. Use a small drop of organic solvent-stable glue to stick the lung to the sample holder. To keep the required penetration depth of the light-sheets as small as possible, set the lung lobe upright. Next, place the sample holder in its chamber.

5.1.3. Set the refractive index of the objective to 3.5 when using ECI as clearing reagent.

5.2. Adjust settings at the light-sheet microscope to detect human cells in the context of the whole organ.

5.2.1. Select required lasers (**filter for measurement > activate checkboxes of required lasers**) and choose appropriate intensities in the control software (**laser transmission control > use slider to set laser intensity > apply**). Use an excitation wavelength of 488 nm (525/50 filter) to detect autofluorescent lung tissue and 640 nm (680/30 filter) to excite human cells labeled with a fluorophore emitting in the red spectrum.

5.2.2. Focus on the sample excited at 488 nm and adapt the focus via the 'chromatic correction' tool at the excitation wavelength of 640 nm (**use the slider to set chromatic correction > apply**).

5.2.3. Choose an appropriate zoom factor; use a low magnification overview (e.g., 6.3x) to determine the overall distribution of labeled cells within the lung tissue and magnified images (e.g., 32x) for detailed localization.

5.2.4. Select a sheet width uniformly elucidating the whole organ or a specific section of interest (**optics > use slider to set sheet width**; usually between 20-40%). Define the sheet numerical aperture (NA) with higher NA creating sharper images (**optics > use slider to set the sheet NA**; for a murine lung lobe expanded to its physiological size a NA of 0.025% can often be used).

5.2.5. Select the number of light-sheets to be used under 'advanced measurement settings'. In case of bidirectional illumination, merge left and right light-sheets to create a homogeneously illuminated image (**advanced measurement > merge lightsheets > select blend mode > use sliders to define overlap between both light-sheets**).

NOTE: It is recommended to take advantage of the bidirectional illumination of the sample with three light-sheets each.

5.2.5.1. To further increase image quality, use the dynamic focus operation. This allows

to move the focus in x-direction during image acquisition.

5.2.6. Define start and end positions of the z-stack to be measured and set the step size to 5 μm (xyz-table Z > scan range).

NOTE: Start and end positions of a z-stack depend on size and positioning of the lung lobe within the sample chamber. However, about 300 to 800 z-stacks are usually acquired for a single lung lobe (5 μm step size).

5.2.7. Save files using 'autosave settings' and start measurement to capture images. After finishing data acquisition, clean the ECi-contaminated sample holder and chamber under running water.

NOTE: Use the same settings to image several lung lobes that are supposed to be compared afterwards.

6. Post-image processing and quantification of lung-accumulated human cells

NOTE: Please see **Table of Materials** for details on the post-imaging software for 3-D analysis, on which the following steps are based. However, alternative post-imaging softwares can be used as well.

6.1. Load the first image of a z-stack (activate the surpass button, file > open > select image) in order to initiate opening of all other images of the chosen z-stack and their automatic 3D reconstruction.

6.2. To ensure correct display of x, y and z dimensions, check voxel sizes and adjust them if necessary (edit > image properties > enter voxel size manually). For the voxel size of z, enter the chosen step-size between two images (here 5 μm).

6.3. Display each channel in a distinct color (edit > show display adjustment). Click on each channel one after the other to define a color of choice (in **Figure 2A,B,C,D** the autofluorescence signal is displayed in grey and labeled human CD4⁺ cells in red).

6.4. Adjust intensity, black level and contrast for each channel (edit > show display adjustment) using the triangles in the channel bars or entering exact numbers in the channel settings. For intensity adjustment, use the right triangle. For black level adjustment, use the left triangle and for contrast adjustment, use the middle triangle.

NOTE: Use the lung derived from the control mouse without cell transfer (step 3.3) to differentiate between specific human cell-derived signals and unspecific background.

6.5. To quantify labeled cells within the pulmonary tissue use 'measurement points' in the toolbar for manual cell counting.

NOTE: Alternatively, select 'spots' for automatic cell counting. However, manual counting allows to differentiate between specific and unspecific signals more precisely.

6.5.1. To compare the accumulation of human cells across different samples, define a lung cube with a specific volume using the 3D cutting tool (**edit > crop 3D**) (here 813 μm x 813 μm x 1000 μm).

6.5.2. Count cells in the 640 nm channel by checking **select** in the pointer menu and mark each cell with a dot via shift-click with the left mouse button. Find the overall number of counted cells displayed in the statistics.

NOTE: It is highly recommended to count several cubes per lung lobe (here five) to ensure reliability of results and compensate for scientist-dependent selection of the counted lung volume (quantification strategy and representative results are depicted in **Figure 2D**).

6.6. Capture an image using the 'snapshot' tool and/or take a video using the 'animation' tool. Save adjusted files as .ims files (**file > export**).

NOTE: For representative purposes, show or hide the frame by checking or unchecking the frame in the toolbar. In addition, display images either as maximal intensity projection (MIP) (**toolbar > volume > mode > check MIP**) or use the 'surface mode' (**toolbar > add new surfaces**). The 'surface mode' has to be activated separately for each channel to highlight tissue architecture and/or cell bodies (representative images are shown in **Figure 2C**).

REPRESENTATIVE RESULTS:

The presented protocol describes an experimental mouse model, which allows monitoring and quantifying the accumulation of adoptively transferred human T lymphocytes in the lung via light-sheet fluorescence microscopy. **Figure 1A** provides a schematic overview of the in vivo steps of the experimental schedule. In order to guarantee reliable results, it is of substantial importance to ensure a good quality of the isolated and fluorescently labeled human CD4⁺ T cells, which will afterwards be transferred into mice. As representatively depicted in **Figure 1B,C**, the above described procedure for microbead-based cell enrichment and subsequent fluorescence-labeling usually results in a flow cytometrically determined CD4⁺ T cell purity > 95% and successful fluorescence-labeling of all CD4⁺ T cells. The quality and penetration depth of light-sheet fluorescence microscopy critically depends on an appropriate grade of tissue clearing. As demonstrated in **Figure 1D**, the here applied protocol for ECI-based tissue clearing was able to guarantee a high level of organ transparency, indicating a successful refractive index matching. Finally, a representative overall result of the described experimental protocol in form of fully processed light-sheet fluorescence microscopy images is demonstrated in **Figure 2B,C,D** and in the **Supplementary Video**. The autofluorescent signal (displayed in grey) provides a helpful tool for imaging the anatomic structure of the lung. The red signal represents lung accumulated human CD4⁺ T cells. Quantification of light-sheet fluorescence microscopy imaging allows determining the overall number of lung accumulated human CD4⁺ T cells per

defined area of inflamed lung tissue. A strategy for quantification of human cell infiltration is illustrated in **Figure 2E**. The (optional) flow cytometric detection of fluorescently labeled cells within the BAL of recipient mice, as depicted in **Figure 2F**, can be used as a supplemental technique in order to confirm the successful tissue migration of adoptively transferred CD4⁺ T cells. Moreover, the preference of transferred human T cells for selective accumulation in inflamed lung tissue in the here described experimental setting was further supported by the fact that human CD4⁺ T cells could not be retrieved in the intestinal mucosa of recipient animals as depicted in **Figure 2B** (right panel).

FIGURE AND TABLE LEGENDS:

Figure 1: Schematic overview of the in vivo experimental workflow.

(A) Allergic lung inflammation was induced in C57BL/6J mice by inhalation of papain (50 µg/mouse) on three consecutive days (d0, d1 and d2). The next day (d3), freshly isolated and fluorescently labeled human CD4⁺ T cells were adoptively transferred into mice via tail vein injection. After another three hours, mice were sacrificed, followed by in situ perfusion and fixation of the lungs. Finally, lungs were explanted and further analyzed ex vivo by light-sheet fluorescence microscopy. Optionally, BAL can be collected before lung explantation to perform extended ex vivo analyses of successfully extravasated and migrated human cells. **(B)** Representative histogram confirming the purity of the isolated CD4⁺ T cell fraction as determined by flow cytometry. Cells stained by an anti-human CD4 antibody or isotype control are displayed in black and grey, respectively. **(C)** Representative histogram confirming the efficacy of the fluorescence-labeling of human CD4⁺ cells prior to adoptive transfer. **(D)** Representative images of a perfused murine lung lobe before and after clearing with ECI. FI, fluorescence intensity.

Figure 2: Representative analysis of the pulmonary accumulation of human CD4⁺ cells in the context of lung inflammation in vivo.

Human CD4⁺ cells were isolated from peripheral blood using density gradient centrifugation followed by a magnetic microbead-based purification step. Human CD4⁺ cells were labeled using a red light-excitable cell proliferation dye and injected intravenously into papain-exposed C57BL/6J mice. After three hours, mice were sacrificed to collect and further analyze the lung tissue via light-sheet fluorescence microscopy. **(A)** Representative overview of a 3D reconstruction of murine, papain-exposed lung tissue (grey) three hours after intravenous injection of labeled human CD4⁺ cells (red) as recorded by light-sheet fluorescence microscopy. **(B)** Lung tissue of a recipient mouse three hours after cell transfer shown as overview or high magnification segment (left panel). Retrieved human CD4⁺ cells could be visualized as red signals and were either depicted in overlay with the autofluorescence signal of lung tissue or as single-channel image. In order to confirm the specificity of the detected signal, control lung tissue without intravenous cell transfer served as negative control (middle panel). In contrast to lung tissue, no labeled human CD4⁺ cells (red) could be detected in the ileum of the same recipient mouse (right panel). **(C)** Post image processing allows analysis of single slices of lung tissue as well as generation of 3D reconstructions of the whole organ segment that can be either represented as maximal intensity projection (MIP) or in surface mode. Representative

images are depicted. **(D)** Quantification strategy is illustrated exemplarily in the same lung as already depicted in Figure 2A. Defined cubes of the analyzed lung segment were selected and the number of human CD4⁺ cells (red) was quantified for each cube. Results of a subsequently performed quantification (events/813 μ m x 813 μ m x 1000 μ m cube) are indicated as mean \pm SEM. **(E)** As an additional option, flow cytometric detection of fluorescently labeled human T cells in the BAL of recipient animals can be performed in order to confirm the successful tissue migration of accumulated human CD4⁺ T cells. BAL cells of the adoptively transferred mouse are displayed in red, BAL cells of a non-transferred control mouse in grey.

Supplementary Video: Representative video sequence showing accumulated human CD4⁺ cells within the murine lung tissue.

3D reconstruction of the murine lung displaying accumulated human CD4⁺ cells (red) within the context of the pulmonary tissue (grey) three hours after intravenous injection into the tail vein. Images are shown as MIP in the beginning and in the surface mode in the end. Images were acquired via light-sheet fluorescence microscopy and processed by post-imaging software for 3D analysis.

DISCUSSION:

The here described experimental setting provides the opportunity to monitor the lung homing capacity of primary human immune cells under in vivo inflammatory conditions and thereby relevantly complements classically performed in vitro adhesion and chemotaxis assays. To take into account specific anatomic organ characteristics of the lung, important aspects of immune cell homing (including chemotaxis and cell distribution within the target organ) as well as the clinical relevance and transferability of acquired data, we took advantage of three technical key features: (1) the analysis of primary human cells within a living murine organism; (2) the papain-mediated induction of pulmonary inflammation; and (3) light-sheet fluorescence microscopy of cleared lung tissue.

Although functional studies of adoptively transferred human immune cells within a living murine organism might be limited in some aspects due to potentially relevant incompatibilities in receptor-ligand-interactions between mice and men, the general concept of humanized mouse models has been established successfully as an important experimental tool in the field of translational medicine during the last decades^{24,32-35}. Compared to classical animal models, studies in humanized mice offer the advantage to directly analyze patient-derived immune cells in an in vivo scenario and thereby to identify functional alterations imprinted by the particular disease^{32,36,37}. Regarding the relevance of potential mismatches between defined receptors on the surface of human immune cells and their respective murine ligands or vice versa, former studies already indicated that human CD4⁺ T cells are able to interact efficiently with the murine adhesion molecules MAdCAM-1 and VCAM-1, which represent crucial ligands for integrin-mediated lymphocyte homing³². Accordingly, migration of intravascularly transferred human immune cells into murine gut tissue could successfully be blocked in vivo by treatment with the clinically used α 4 β 7 integrin antibody vedolizumab³². However, even in case that a specific receptor-ligand-interaction of relevance might show a complete human/murine mismatch, it will presumably be possible to overcome this limitation by genetic engineering

and, for instance, by transgenic overexpression of the respective human ligand, growth factor, cytokine or receptor within the murine organism^{33,35}.

As a significant influence of chronic inflammation on the local secretion of chemokines, the endothelial expression of adhesion molecules and the subsequent accumulation of lymphocytes has been described in numerous publications³⁸⁻⁴⁰, the choice of a suitable experimental model of pulmonary inflammation represented a critical step while establishing the above described protocol and might be adapted dependent on the clinical context of each individual study. The here selected setting of papain-induced allergic lung inflammation represents a well-described experimental model, which is based on the capacity of the locally administered cysteine protease papain to irritate the airway epithelium and trigger the subsequent release of alarmins^{27,41,42}. Interestingly, accidental exposition to papain is known to cause asthma development in humans as well⁴³. Dependent on the inhaled dose of papain, exposed mice show an accumulation of innate and adaptive immune cells and elevated levels of type 2 cytokines in the lung²⁷. While dose escalation turned out to result in an enlargement of airspaces (classic histological phenomenon of COPD) and a destruction of blood vessel walls with subsequent hemorrhage, moderate dosing schedules went along with a prominent pulmonary eosinophilia and thus mimicked an important histological feature of human asthma²⁷. As our purpose was to use this experimental model to generate an inflammatory context for the analysis of pulmonary immune cell homing, we carefully tried to avoid papain-induced damage of blood vessels, which might otherwise result in an unphysiological extravasation of human immune cells due to disturbed endothelial integrity. Accordingly, we selected an intermediate dose of 50 µg of papain per mouse per day in the above described protocol. Although development of papain-induced airway inflammation also occurs in the absence of B and T lymphocytes, lung infiltrating adaptive immune cells are known to impact significantly on the course of disease^{27,42}. For instance, regulatory T cells could be identified as potent regulators of papain-induced airway eosinophilia²⁷. In perspective, the active involvement of pulmonary lymphocytes in the inflammatory pathogenesis of papain-exposed mice implicates that the above described protocol might in addition enable to analyze the functional capacity of adoptively transferred and successfully lung-accumulated human immune cells to modulate lung pathology (e.g., via flow cytometric acquisition of eosinophilic counts in BAL). Furthermore, an additionally performed intranasal administration of selected disease-relevant human chemokines just prior to intravascular cell transfer might allow to analyze the impact of these humoral mediators on the lung homing process of distinct human immune cell populations in an in vivo setting. Likewise, the effect of inhibitors on the lung homing process and, subsequently, on inflammatory lung pathology can be studied.

A particular advantage of the here introduced experimental procedure is the precise tracking and localization of lung infiltrating human immune cells by the high-end imaging quality of light-sheet fluorescence microscopy. Recent studies already demonstrated that the technique of light-sheet fluorescence microscopy represents a valuable experimental tool for analysis of intestinal immune cell homing in translational IBD research and is able to overcome the main limitations of conventional immunofluorescence microscopy and flow cytometry^{24,32}. While analyses based on conventional microscopy are usually restricted to a very small and potentially

not representative area of the organ and flow cytometry does not take into account the aspect of tissue organization at all, light-sheet fluorescence microscopy of chemically cleared tissue allows an increased penetration depth without major loss of resolution and thus enables a 3D reconstruction of rather large organ sections (up to 1.5 cm x 1.5 cm)^{24,28,44}. For sure, the quality and validity of acquired 3D reconstructions critically depend on the performance of tissue clearance. In the here described setting, we included a slightly adopted version of the recently published protocol for ECI-based tissue clearing⁴⁴. Compared to other well established strategies for solvent-based tissue clearing^{26,45,46}, the ECI-based protocol combines the advantages of excellent clearing properties, low toxicity of used reagents and a moderate time requirement⁴⁴. As the capacity of standard light-sheet fluorescence microscopy to resolve finest tissue structures like alveolar capillaries is still limited even under optimal clearing conditions²⁸, it might somehow be difficult to reliably differentiate between intravascular and already extravasated immune cells. The inclusion of an additional standard fluorescence-based blood vessel staining into the here described protocol would most probably not be able to fully overcome this limitation. Thus, studies with a particular focus on the behavior of immune cells within the pulmonary microcirculation or their diapedesis might preferentially take into account a recently published and very elegant protocol for intravital lung imaging based on 2-photon microscopy⁴⁷. In this experimental setting, a thoracic window was implanted into anesthetized and ventilated mice, through which the stabilized lung can be monitored by a resonant-scanning 2-photon microscopy module, allowing high-resolution imaging throughout the respiratory cycle upon preserved ventilation and perfusion^{47,48}. This technique has been successfully applied in various studies and was able to visualize for instance intrapulmonary platelet biogenesis and the lung entrance of circulating tumor cells^{49,50}. However, besides the requirement of sophisticated instrumental equipment (e.g., mouse ventilation system) and the need of extensive invasive manipulations in living animals (implantation of the thoracic window and intravital microscopy), the main limitation of this live lung microscopy system is the confined z-axis penetration. The performed lung surface imaging only allows analyzing the outer 100 μ m of subpleural lung tissue^{47,48}. Dependent on the scientific context, it might be a valuable option to implement 2-photon microscopy of the explanted lungs as an additional procedure into the above described protocol. Analyzing the same lung first by 2-photon microscopy and afterwards by light-sheet fluorescence microscopy might represent a strategy to obtain a quantitative overview of the distribution and localization of human immune cells within the murine lung (light-sheet fluorescence microscopy) and, at the same time, gain more detailed insights into cellular or microvascular processes (2-photon microscopy). Indeed, 2-photon microscopy of murine tracheal explants represents an established imaging tool for analyzing immune cell behavior in the context of experimentally induced lung inflammation^{51,52}. Instead of visualizing small pulmonary capillaries, the successful extravasation and lung tissue infiltration of the transferred human T cells in our experimental model can also be proven by detecting fluorescently labeled human cells within the BAL of recipient animals via flow cytometry as exemplarily depicted in **Figure 2E**. In general, analyses of the cellular BAL compartment represent a well-established method to characterize the pulmonary immune cell influx in the context of inflammatory respiratory diseases³¹. Finally, another flow cytometric strategy for quantifying the extravasation of adoptively transferred immune cells within lung tissue was described by Galkina et al. (2005)⁵³ and could potentially be combined with the here

described protocol. In the study by Galkina et al., a single intravenous injection of a fluorescence-conjugated anti-CD8 antibody shortly before resection of the lung resulted in an exclusive and complete labeling of before transferred CD8⁺ T cells within the lung vascular compartment, while already extravasated CD8⁺ T cells within the lung interstitium remained unstained. Subsequent analyses of in vivo labeled pulmonary immune cells were performed flow cytometrically after *ex vivo* digestion of lung tissue⁵³. Of course, the process of tissue digestion means that the anatomic separation between the intra- and extravascular lung compartment is abrogated and, thus, there is a general risk of false-positive labeling of interstitial immune cells due to antibody leakage between both compartments. This risk can only be minimized by performing the tissue digestion in the presence of saturating amounts of unlabeled antibody⁵³ or, potentially, by replacing flow cytometric analysis by light-sheet fluorescence microscopy, which makes it possible to completely avoid the destruction of tissue structure.

In summary, the here introduced combination of in vivo fluorescence cell labeling and subsequent light-sheet fluorescence microscopy is able to reliably identify, quantify and localize lung accumulated human immune cells in an experimental mouse model of pulmonary inflammation.

ACKNOWLEDGMENTS:

The authors gratefully acknowledge funding by the DFG Collaborative Research Centers SFB 1181 and TRR 241. The Optical Imaging Centre Erlangen (OICE) and in particular Ralf Palmisano, Philipp Tripal and Tina Fraaß (Project Z2 of the DFG CRC 1181) are acknowledged for expert technical support for light-sheet fluorescence microscopic imaging.

DISCLOSURES:

M.F. Neurath has served as an advisor for Pentax, Giuliani, MSD, Abbvie, Janssen, Takeda and Boehringer. The remaining authors do not disclose any conflict.

REFERENCES:

- 1 Medoff, B. D., Thomas, S. Y., Luster, A. D. T cell trafficking in allergic asthma: the ins and outs. *Annual Review of Immunology*. **26**, 205-232, doi:10.1146/annurev.immunol.26.021607.090312 (2008).
- 2 Baraldo, S., Lokar Oliani, K., Turato, G., Zuin, R., Saetta, M. The Role of Lymphocytes in the Pathogenesis of Asthma and COPD. *Current Medicinal Chemistry*. **14** (21), 2250-2256 (2007).
- 3 Mikhak, Z., Strassner, J. P., Luster, A. D. Lung dendritic cells imprint T cell lung homing and promote lung immunity through the chemokine receptor CCR4. *Journal of Experimental Medicine*. **210** (9), 1855-1869, doi:10.1084/jem.20130091 (2013).
- 4 Thomas, S. Y., Banerji, A., Medoff, B. D., Lilly, C. M., Luster, A. D. Multiple chemokine receptors, including CCR6 and CXCR3, regulate antigen-induced T cell homing to the human asthmatic airway. *Journal of Immunology*. **179** (3), 1901-1912 (2007).
- 5 Katchar, K., Eklund, A., Grunewald, J. Expression of Th1 markers by lung accumulated T cells in pulmonary sarcoidosis. *Journal of Internal Medicine*. **254** (6), 564-571 (2003).
- 6 Wu, Z. et al. Mast cell FcεpsilonRI-induced early growth response 2 regulates CC

705 chemokine ligand 1-dependent CD4⁺ T cell migration. *Journal of Immunology*. **190** (9), 4500-
706 4507, doi:10.4049/jimmunol.1203158 (2013).

707 7 Hart, P. H. Regulation of the inflammatory response in asthma by mast cell products.
708 *Immunology, Cell Biology*. **79** (2), 149-153, doi:10.1046/j.1440-1711.2001.00983.x (2001).

709 8 Bice, J. B., Leechawengwongs, E., Montanaro, A. Biologic targeted therapy in allergic
710 asthma. *Annals of Allergy & Asthma & Immunology*. **112** (2), 108-115,
711 doi:10.1016/j.anai.2013.12.013 (2014).

712 9 Barnes, N. et al. A randomized, double-blind, placebo-controlled study of the CRTH2
713 antagonist OC000459 in moderate persistent asthma. *Clinical & Experimental Allergy*. **42** (1),
714 38-48, doi:10.1111/j.1365-2222.2011.03813.x (2012).

715 10 Medoff, B. D. et al. CD11b⁺ myeloid cells are the key mediators of Th2 cell homing into
716 the airway in allergic inflammation. *Journal of Immunology*. **182** (1), 623-635 (2009).

717 11 Oeser, K., Maxeiner, J., Symowski, C., Stassen, M., Voehringer, D. T cells are the critical
718 source of IL-4/IL-13 in a mouse model of allergic asthma. *Allergy*. **70** (11), 1440-1449,
719 doi:10.1111/all.12705 (2015).

720 12 Freeman, C. M., Curtis, J. L., Chensue, S. W. CC chemokine receptor 5 and CXC
721 chemokine receptor 6 expression by lung CD8⁺ cells correlates with chronic obstructive
722 pulmonary disease severity. *The American Journal of Pathology*. **171** (3), 767-776,
723 doi:10.2353/ajpath.2007.061177 (2007).

724 13 Kallinich, T. et al. Chemokine-receptor expression on T cells in lung compartments of
725 challenged asthmatic patients. *Clinical & Experimental Allergy*. **35** (1), 26-33,
726 doi:10.1111/j.1365-2222.2004.02132.x (2005).

727 14 Vasakova, M. et al. Bronchoalveolar lavage fluid cellular characteristics, functional
728 parameters and cytokine and chemokine levels in interstitial lung diseases. *Scandinavian*
729 *Journal of Immunology*. **69** (3), 268-274, doi:10.1111/j.1365-3083.2008.02222.x (2009).

730 15 Campbell, J. J. et al. Expression of chemokine receptors by lung T cells from normal and
731 asthmatic subjects. *Journal of Immunology*. **166** (4), 2842-2848 (2001).

732 16 Halwani, R. et al. IL-17 Enhances Chemotaxis of Primary Human B Cells during Asthma.
733 *PLoS One*. **9** (12), e114604, doi:10.1371/journal.pone.0114604 (2014).

734 17 Agostini, C. et al. Cxcr3 and its ligand CXCL10 are expressed by inflammatory cells
735 infiltrating lung allografts and mediate chemotaxis of T cells at sites of rejection. *The American*
736 *Journal of Pathology*. **158** (5), 1703-1711, doi:10.1016/S0002-9440(10)64126-0 (2001).

737 18 Ainslie, M. P., McNulty, C. A., Huynh, T., Symon, F. A., Wardlaw, A. J. Characterisation of
738 adhesion receptors mediating lymphocyte adhesion to bronchial endothelium provides
739 evidence for a distinct lung homing pathway. *Thorax*. **57** (12), 1054-1059 (2002).

740 19 Radeke, H. H., Ludwig, R. J., Boehncke, W. H. Experimental approaches to lymphocyte
741 migration in dermatology in vitro and in vivo. *Experimental Dermatology*. **14** (9), 641-666,
742 doi:10.1111/j.0906-6705.2005.00350.x (2005).

743 20 Miles, A., Liaskou, E., Eksteen, B., Lalor, P. F., Adams, D. H. CCL25 and CCL28 promote
744 alpha4 beta7-integrin-dependent adhesion of lymphocytes to MAdCAM-1 under shear flow.
745 *American Journal of Physiology-Gastrointestinal and Liver Physiology*. **294** (5), G1257-1267,
746 doi:10.1152/ajpgi.00266.2007 (2008).

747 21 Zundler, S. et al. The alpha4beta1 Homing Pathway Is Essential for Ileal Homing of
748 Crohn's Disease Effector T Cells In vivo. *Inflammatory Bowel Diseases*. **23** (3), 379-391,

doi:10.1097/MIB.0000000000001029 (2017).

22 Verbist, K. C., Cole, C. J., Field, M. B., Klonowski, K. D. A role for IL-15 in the migration of effector CD8 T cells to the lung airways following influenza infection. *Journal of Immunology*. **186** (1), 174-182, doi:10.4049/jimmunol.1002613 (2011).

23 Kopf, M., Abel, B., Gallimore, A., Carroll, M., Bachmann, M. F. Complement component C3 promotes T-cell priming and lung migration to control acute influenza virus infection. *Nature Medicine*. **8** (4), 373-378, doi:10.1038/nm0402-373 (2002).

24 Zundler, S. et al. Three-Dimensional Cross-Sectional Light-Sheet Microscopy Imaging of the Inflamed Mouse Gut. *Gastroenterology*. **153** (4), 898-900, doi:10.1053/j.gastro.2017.07.022 (2017).

25 Mzinza, D. T. et al. Application of light sheet microscopy for qualitative and quantitative analysis of bronchus-associated lymphoid tissue in mice. *Cellular & Molecular Immunology*. doi:10.1038/cmi.2017.150 (2018).

26 Erturk, A., Lafkas, D., Chalouni, C. Imaging cleared intact biological systems at a cellular level by 3DISCO. *Journal of Visualized Experiments*. (89), doi:10.3791/51382 (2014).

27 Morita, H. et al. An Interleukin-33-Mast Cell-Interleukin-2 Axis Suppresses Papain-Induced Allergic Inflammation by Promoting Regulatory T Cell Numbers. *Immunity*. **43** (1), 175-186, doi:10.1016/j.immuni.2015.06.021 (2015).

28 Mann, L., Klingberg, A., Gunzer, M., Hasenberg, M. Quantitative Visualization of Leukocyte Infiltrate in a Murine Model of Fulminant Myocarditis by Light Sheet Microscopy. *Journal of Visualized Experiments*. (123), doi:10.3791/55450 (2017).

29 Mercer, R. R. et al. Extrapulmonary transport of MWCNT following inhalation exposure. *Particle and Fibre Toxicology*. **10** 38, doi:10.1186/1743-8977-10-38 (2013).

30 Minton, C. et al. Demonstration of microvessel networks and endothelial cell phenotypes in the normal murine lung. *Journal of Nippon Medical School*. **72** (6), 314-315 (2005).

31 Van Hoecke, L., Job, E. R., Saelens, X., Roose, K. Bronchoalveolar Lavage of Murine Lungs to Analyze Inflammatory Cell Infiltration. *Journal of Visualized Experiments*. (123), doi:10.3791/55398 (2017).

32 Fischer, A. et al. Differential effects of alpha4beta7 and GPR15 on homing of effector and regulatory T cells from patients with UC to the inflamed gut in vivo. *Gut*. **65** (10), 1642-1664, doi:10.1136/gutjnl-2015-310022 (2016).

33 Shultz, L. D., Ishikawa, F., Greiner, D. L. Humanized mice in translational biomedical research. *Nature Reviews Immunology*. **7** (2), 118-130, doi:10.1038/nri2017 (2007).

34 Brehm, M. A., Jouvett, N., Greiner, D. L., Shultz, L. D. Humanized mice for the study of infectious diseases. *Current Opinion in Immunology*. **25** (4), 428-435, doi:10.1016/j.coi.2013.05.012 (2013).

35 Wege, A. K. Humanized Mouse Models for the Preclinical Assessment of Cancer Immunotherapy. *BioDrugs*. doi:10.1007/s40259-018-0275-4 (2018).

36 Jespersen, H. et al. Clinical responses to adoptive T-cell transfer can be modeled in an autologous immune-humanized mouse model. *Nature Communications*. **8** (1), 707, doi:10.1038/s41467-017-00786-z (2017).

37 Schloder, J., Berges, C., Luessi, F., Jonuleit, H. Dimethyl Fumarate Therapy Significantly Improves the Responsiveness of T Cells in Multiple Sclerosis Patients for Immunoregulation by

793 Regulatory T Cells. *International Journal of Molecular Sciences*. **18** (2),
794 doi:10.3390/ijms18020271 (2017).

795 38 Murdoch, C., Finn, A. Chemokine receptors and their role in inflammation and infectious
796 diseases. *Blood*. **95** (10), 3032-3043 (2000).

797 39 Rivera-Nieves, J., Gofu, G., Ley, K. Leukocyte adhesion molecules in animal models of
798 inflammatory bowel disease. *Inflammatory Bowel Diseases*. **14** (12), 1715-1735,
799 doi:10.1002/ibd.20501 (2008).

800 40 Zundler, S., Neurath, M. F. Novel Insights into the Mechanisms of Gut Homing and
801 Antiadhesion Therapies in Inflammatory Bowel Diseases. *Inflammatory Bowel Diseases*. **23** (4),
802 617-627, doi:10.1097/MIB.0000000000001067 (2017).

803 41 Halim, T. Y., Krauss, R. H., Sun, A. C., Takei, F. Lung natural helper cells are a critical
804 source of Th2 cell-type cytokines in protease allergen-induced airway inflammation. *Immunity*.
805 **36** (3), 451-463, doi:10.1016/j.immuni.2011.12.020 (2012).

806 42 Kamijo, S. et al. IL-33-mediated innate response and adaptive immune cells contribute
807 to maximum responses of protease allergen-induced allergic airway inflammation. *Journal of*
808 *Immunology*. **190** (9), 4489-4499, doi:10.4049/jimmunol.1201212 (2013).

809 43 Milne, J., Brand, S. Occupational asthma after inhalation of dust of the proteolytic
810 enzyme, papain. *British Journal of Industrial Medicine*. **32** (4), 302-307 (1975).

811 44 Klingberg, A. et al. Fully Automated Evaluation of Total Glomerular Number and
812 Capillary Tuft Size in Nephritic Kidneys Using Lightsheet Microscopy. *Journal of the American*
813 *Society of Nephrology*. **28** (2), 452-459, doi:10.1681/ASN.2016020232 (2017).

814 45 Ariel, P. A beginner's guide to tissue clearing. *The International Journal of Biochemistry,*
815 *Cell Biology*. **84** 35-39, doi:10.1016/j.biocel.2016.12.009 (2017).

816 46 Richardson, D. S., Lichtman, J. W. Clarifying Tissue Clearing. *Cell*. **162** (2), 246-257,
817 doi:10.1016/j.cell.2015.06.067 (2015).

818 47 Looney, M. R. et al. Stabilized imaging of immune surveillance in the mouse lung. *Nature*
819 *Methods*. **8** (1), 91-96, doi:10.1038/nmeth.1543 (2011).

820 48 Looney, M. R., Bhattacharya, J. Live imaging of the lung. *Annual Review of Physiology*. **76**
821 431-445, doi:10.1146/annurev-physiol-021113-170331 (2014).

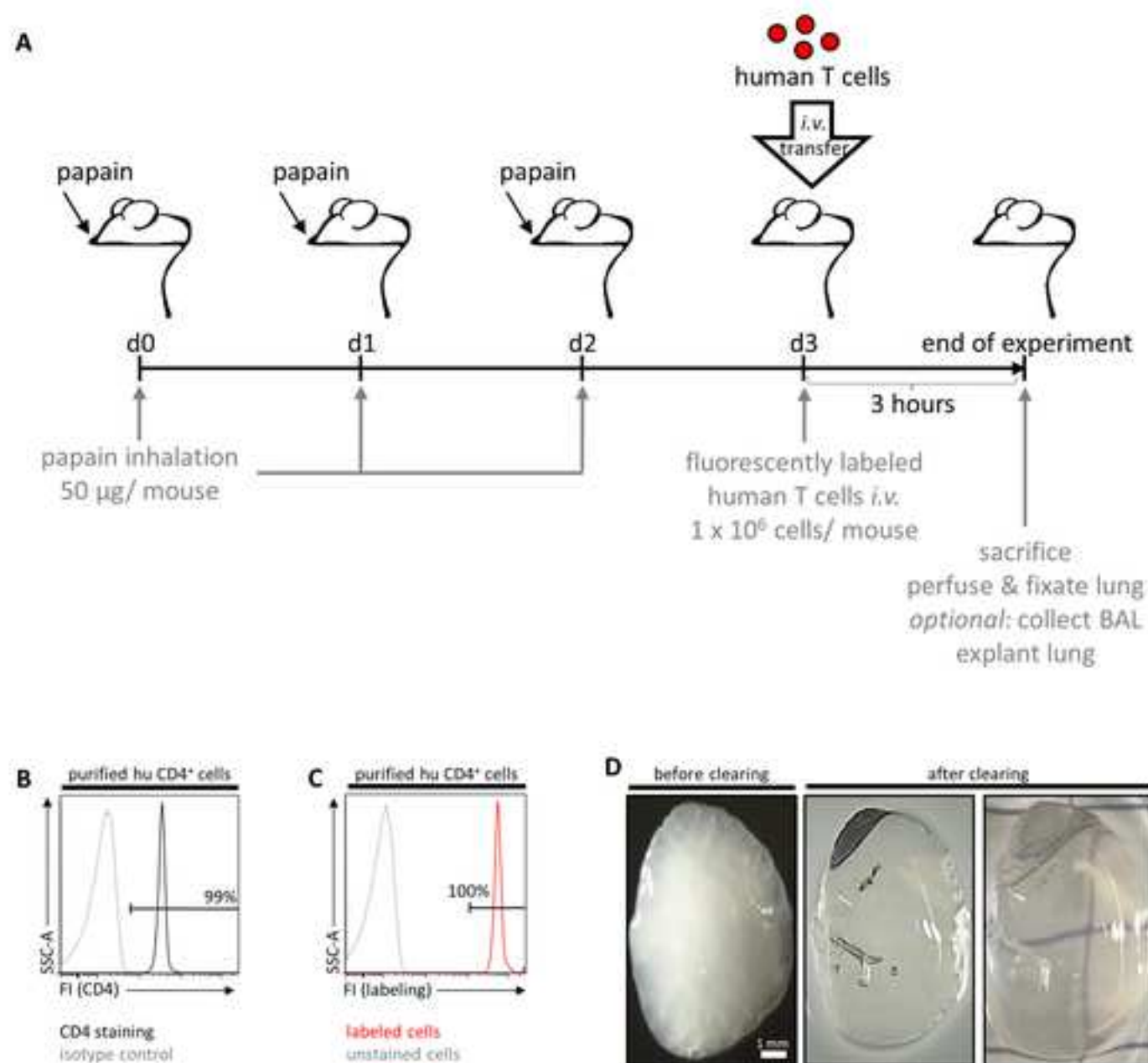
822 49 Lefrancais, E. et al. The lung is a site of platelet biogenesis and a reservoir for
823 haematopoietic progenitors. *Nature*. **544** (7648), 105-109, doi:10.1038/nature21706 (2017).

824 50 Headley, M. B. et al. Visualization of immediate immune responses to pioneer
825 metastatic cells in the lung. *Nature*. **531** (7595), 513-517, doi:10.1038/nature16985 (2016).

826 51 Hammad, H. et al. House dust mite allergen induces asthma via Toll-like receptor 4
827 triggering of airway structural cells. *Nature Medicine*. **15** (4), 410-416, doi:10.1038/nm.1946
828 (2009).

829 52 Bose, O. et al. Mast cells present protrusions into blood vessels upon tracheal allergen
830 challenge in mice. *PLoS One*. **10** (3), e0118513, doi:10.1371/journal.pone.0118513 (2015).

831 53 Galkina, E. et al. Preferential migration of effector CD8+ T cells into the interstitium of
832 the normal lung. *Journal of Clinical Investigation*. **115** (12), 3473-3483, doi:10.1172/JCI24482
833 (2005).

**Figure 1**

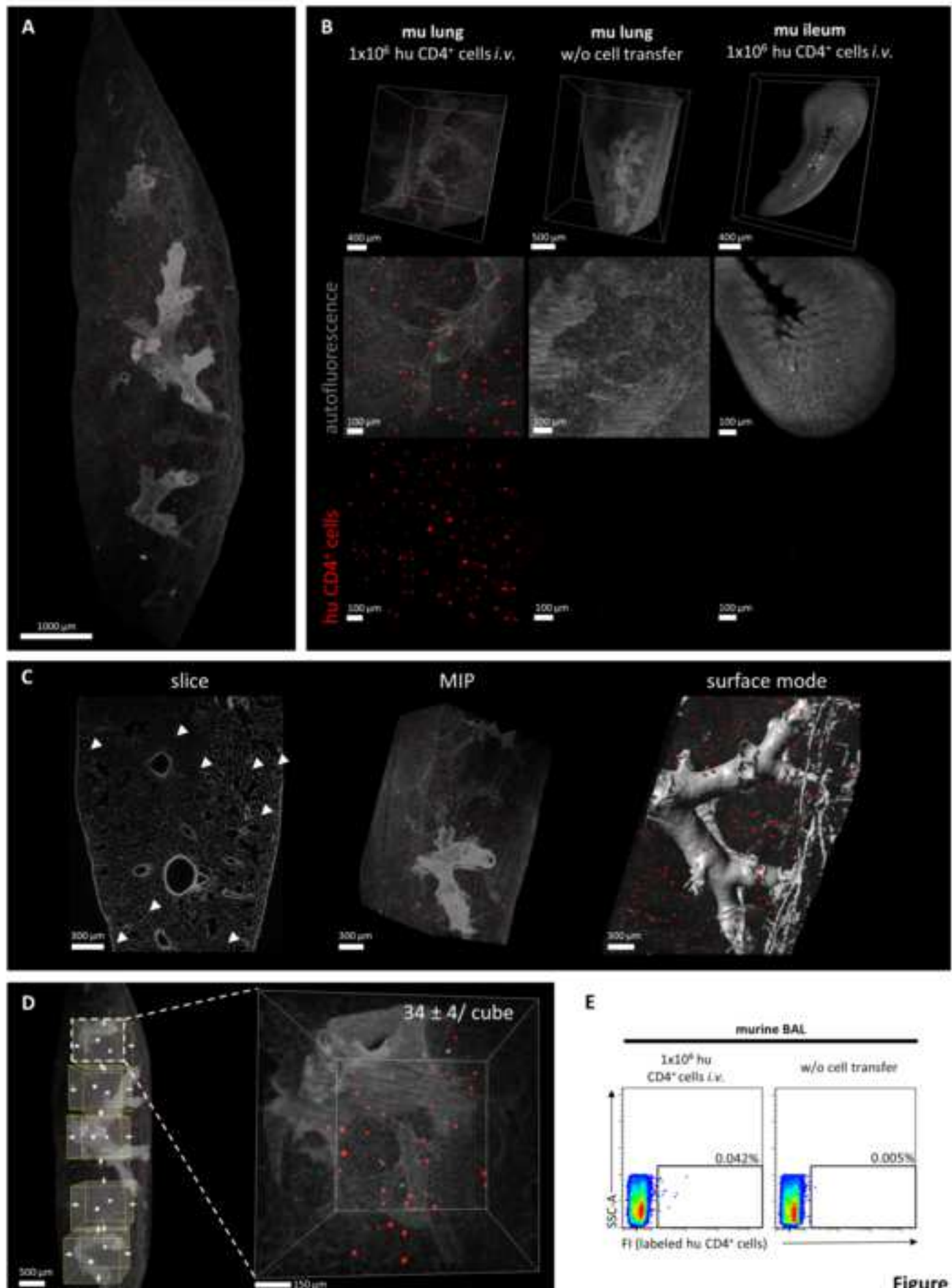


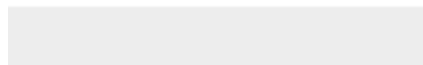
Figure 2



[Click here to access/download](#)

Video or Animated Figure

Schulz-Kuhnt_supplementary video.mp4



Name of Material/ Equipment	Company	Catalog Number	Comments/Description
Agarose NEEO Ultra	Carl Roth GmbH + Co. KG, Karlsruhe, Germany	2267.4	
AlexaFlour594 anti-human CD45 antibody	BioLegend, San Diego, USA	304060	
Ammonium chloride	Carl Roth GmbH + Co. KG, Karlsruhe, Germany	K2981	
Cannula 21 G	Becton, Dickinson and Company, Franklin Lakes, USA	301300	
Cell proliferation dye eflour670	eBioscience Inc., San Diego, USA	65-0840-85	
CD4 MicroBeads, human	Miltenyi Biotech GmbH, Bergisch-Gladbach, Germany	130-045-101	
EDTA (ethylenediaminetetraacetic acid)	Carl Roth GmbH + Co. KG, Karlsruhe, Germany	8043.1	
Potassium-EDTA blood collection tube, 9 ml	Sarstedt AG & Co., Nümbrecht, Germany	21066001	
Ethly cinnamate (ECi)	Sigma-Aldrich, Steinheim, Germany	112372-100G	
Ethanol ≥ 99.5 % (EtOH)	Carl Roth GmbH + Co. KG, Karlsruhe, Germany	5054.3	
FBS (fetal bovine serum) Good Forte	PAN-Biotech GmbH, Aidenbach, Germany	P40-47500	
Filter 100 µm	VWR International Germany GmbH, Darmstadt, Germany	732-2758	
Imaris Image Analysis Software 9.0.2	Bitplane AG, Zurich, Switzerland	n.a.	
ImspectroPro software	Abberior Instruments GmbH, Göttingen, Germany	n.a.	
Ketamin	Inresa Arzneimittel GmbH, Freiburg, Germany	3617KET-V	
LaVision UltraMicroscope II	LaVision BioTec GmbH, Bielefeld, Germany	n.a.	
MACS MultiStand	Miltenyi Biotech GmbH, Bergisch-Gladbach, Germany	130-042-303	
Multitly cannula 20 G	Sarstedt AG & Co., Nümbrecht, Germany	851638035	
30 G needle	B. Braun Melsungen AG, Melsungen, Hessen, Germany	9161502	
Neubauer counting chamber	neoLab Migge GmbH, Heidelberg, Germany	C-1003	
Pattex Glue	Henkel AG & Co, Düsseldorf, Germany	PSK1C	
LS column	Miltenyi Biotech GmbH, Bergisch-Gladbach, Germany	130-042-401	
Lymphocyte Separation Media (Density 1,077 g/ml)	anprotec	AC-AF-0018	
RPMI medium	(Gibco) Life Technologies GmbH, Darmstadt, Germany	61870-010	
Papain	Merck	1,071,440,025	
PBS Dulbecco (phosphate buffered saline)	Biochrom GmbH, Berlin, Germany	L182-10	
PerCP/Cy5.5 anti-human CD4	BioLegend, San Diego, USA	317428	
PerCP/Cy5.5 mouse IgG2b, κ isotype Ctrl	BioLegend, San Diego, USA	400337	
PFA (paraformaldehyde)	Carl Roth GmbH + Co. KG, Karlsruhe, Germany	0335.1	
Potassium hydrogen carbonate	Carl Roth GmbH + Co. KG, Karlsruhe, Germany	P7481	
Serological pipette 10 ml	Sarstedt AG & Co., Nümbrecht, Germany	86.1254.001	
Syringe 1 ml	B. Braun Melsungen AG, Melsungen, Hessen, Germany	9166017V	
Syringe 5 ml	Becton, Dickinson and Company, Franklin Lakes, USA	260067	
Syringe 20 ml	Becton, Dickinson and Company, Franklin Lakes, USA	260069	
Tube 1.5 ml	Sarstedt AG & Co., Nümbrecht, Germany	72,706,400	
Tube 2 ml	Sarstedt AG & Co., Nümbrecht, Germany	72.695.400	
Tube 2 ml, brown	Sarstedt AG & Co., Nümbrecht, Germany	72,695,001	
Tube 15 ml	Sarstedt AG & Co., Nümbrecht, Germany	62.554.502	
Tube 50 ml	Sarstedt AG & Co., Nümbrecht, Germany	62.547.254	
QuadroMACS Separator	Miltenyi Biotech GmbH, Bergisch-Gladbach, Germany	130-090-976	
Xylazin (Rompun 2%)	Bayer Vital GmbH, Leverkusen, Germany	KPOBD32	



1 Alewife Center #200
Cambridge, MA 02140
tel. 617.945.9051
www.jove.com

ARTICLE AND VIDEO LICENSE AGREEMENT

Title of Article:

Quantitative Imaging of Lung homing human Lymphocytes in a humanized mouse model of allergic inflammation based on Light-sheet fluorescence microscopy

Author(s):

Anja Schulz-Kuhnt, Sebastian Dunder, Anika Güneboom, Clemens Neufert, Stefan Witz, Markus F. Newath, Imke Ataya

Item 1 (check one box): The Author elects to have the Materials be made available (as described at <http://www.jove.com/author>) via: ☒ Standard Access ☐ Open Access

Item 2 (check one box):

- ☒ The Author is NOT a United States government employee.
☐ The Author is a United States government employee and the Materials were prepared in the course of his or her duties as a United States government employee.
☐ The Author is a United States government employee but the Materials were NOT prepared in the course of his or her duties as a United States government employee.

ARTICLE AND VIDEO LICENSE AGREEMENT

1. **Defined Terms.** As used in this Article and Video License Agreement, the following terms shall have the following meanings: "**Agreement**" means this Article and Video License Agreement; "**Article**" means the article specified on the last page of this Agreement, including any associated materials such as texts, figures, tables, artwork, abstracts, or summaries contained therein; "**Author**" means the author who is a signatory to this Agreement; "**Collective Work**" means a work, such as a periodical issue, anthology or encyclopedia, in which the Materials in their entirety in unmodified form, along with a number of other contributions, constituting separate and independent works in themselves, are assembled into a collective whole; "**CRC License**" means the Creative Commons Attribution-Non Commercial-No Derivs 3.0 Unported Agreement, the terms and conditions of which can be found at: <http://creativecommons.org/licenses/by-nc-nd/3.0/legalcode>; "**Derivative Work**" means a work based upon the Materials or upon the Materials and other pre-existing works, such as a translation, musical arrangement, dramatization, fictionalization, motion picture version, sound recording, art reproduction, abridgment, condensation, or any other form in which the Materials may be recast, transformed, or adapted; "**Institution**" means the institution, listed on the last page of this Agreement, by which the Author was employed at the time of the creation of the Materials; "**JoVE**" means MyJoVE Corporation, a Massachusetts corporation and the publisher of *The Journal of Visualized Experiments*; "**Materials**" means the Article and / or the Video; "**Parties**" means the Author and JoVE; "**Video**" means any video(s) made by the Author, alone or in conjunction with any other parties, or by JoVE or its affiliates or agents, individually or in collaboration with the Author or any other parties, incorporating all or any portion of the Article, and in which the Author may or may not appear.

2. **Background.** The Author, who is the author of the Article, in order to ensure the dissemination and protection of the Article, desires to have the JoVE publish the Article and create and transmit videos based on the Article. In furtherance of such goals, the Parties desire to memorialize in this Agreement the respective rights of each Party in and to the Article and the Video.

3. **Grant of Rights in Article.** In consideration of JoVE agreeing to publish the Article, the Author hereby grants to JoVE, subject to **Sections 4 and 7** below, the exclusive, royalty-free, perpetual (for the full term of copyright in the Article, including any extensions thereto) license (a) to publish, reproduce, distribute, display and store the Article in all forms, formats and media whether now known or hereafter developed (including without limitation in print, digital and electronic form) throughout the world, (b) to translate the Article into other languages, create adaptations, summaries or extracts of the Article or other Derivative Works (including, without limitation, the Video) or Collective Works based on all or any portion of the Article and exercise all of the rights set forth in (a) above in such translations, adaptations, summaries, extracts, Derivative Works or Collective Works and (c) to license others to do any or all of the above. The foregoing rights may be exercised in all media and formats, whether now known or hereafter devised, and include the right to make such modifications as are technically necessary to exercise the rights in other media and formats. If the "Open Access" box has been checked in **Item 1** above, JoVE and the Author hereby grant to the public all such rights in the Article as provided in, but subject to all limitations and requirements set forth in, the CRC License.

ARTICLE AND VIDEO LICENSE AGREEMENT

4. **Retention of Rights in Article.** Notwithstanding the exclusive license granted to JoVE in **Section 3** above, the Author shall, with respect to the Article, retain the non-exclusive right to use all or part of the Article for the non-commercial purpose of giving lectures, presentations or teaching classes, and to post a copy of the Article on the Institution's website or the Author's personal website, in each case provided that a link to the Article on the JoVE website is provided and notice of JoVE's copyright in the Article is included. All non-copyright intellectual property rights in and to the Article, such as patent rights, shall remain with the Author.

5. **Grant of Rights in Video – Standard Access.** This **Section 5** applies if the "Standard Access" box has been checked in **Item 1** above or if no box has been checked in **Item 1** above. In consideration of JoVE agreeing to produce, display or otherwise assist with the Video, the Author hereby acknowledges and agrees that, Subject to **Section 7** below, JoVE is and shall be the sole and exclusive owner of all rights of any nature, including, without limitation, all copyrights, in and to the Video. To the extent that, by law, the Author is deemed, now or at any time in the future, to have any rights of any nature in or to the Video, the Author hereby disclaims all such rights and transfers all such rights to JoVE.

6. **Grant of Rights in Video – Open Access.** This **Section 6** applies only if the "Open Access" box has been checked in **Item 1** above. In consideration of JoVE agreeing to produce, display or otherwise assist with the Video, the Author hereby grants to JoVE, subject to **Section 7** below, the exclusive, royalty-free, perpetual (for the full term of copyright in the Article, including any extensions thereto) license (a) to publish, reproduce, distribute, display and store the Video in all forms, formats and media whether now known or hereafter developed (including without limitation in print, digital and electronic form) throughout the world, (b) to translate the Video into other languages, create adaptations, summaries or extracts of the Video or other Derivative Works or Collective Works based on all or any portion of the Video and exercise all of the rights set forth in (a) above in such translations, adaptations, summaries, extracts, Derivative Works or Collective Works and (c) to license others to do any or all of the above. The foregoing rights may be exercised in all media and formats, whether now known or hereafter devised, and include the right to make such modifications as are technically necessary to exercise the rights in other media and formats. For any Video to which this **Section 6** is applicable, JoVE and the Author hereby grant to the public all such rights in the Video as provided in, but subject to all limitations and requirements set forth in, the CRC License.

7. **Government Employees.** If the Author is a United States government employee and the Article was prepared in the course of his or her duties as a United States government employee, as indicated in **Item 2** above, and any of the licenses or grants granted by the Author hereunder exceed the scope of the 17 U.S.C. 403, then the rights granted hereunder shall be limited to the maximum rights permitted under such

statute. In such case, all provisions contained herein that are not in conflict with such statute shall remain in full force and effect, and all provisions contained herein that do so conflict shall be deemed to be amended so as to provide to JoVE the maximum rights permissible within such statute.

8. **Likeness, Privacy, Personality.** The Author hereby grants JoVE the right to use the Author's name, voice, likeness, picture, photograph, image, biography and performance in any way, commercial or otherwise, in connection with the Materials and the sale, promotion and distribution thereof. The Author hereby waives any and all rights he or she may have, relating to his or her appearance in the Video or otherwise relating to the Materials, under all applicable privacy, likeness, personality or similar laws.

9. **Author Warranties.** The Author represents and warrants that the Article is original, that it has not been published, that the copyright interest is owned by the Author (or, if more than one author is listed at the beginning of this Agreement, by such authors collectively) and has not been assigned, licensed, or otherwise transferred to any other party. The Author represents and warrants that the author(s) listed at the top of this Agreement are the only authors of the Materials. If more than one author is listed at the top of this Agreement and if any such author has not entered into a separate Article and Video License Agreement with JoVE relating to the Materials, the Author represents and warrants that the Author has been authorized by each of the other such authors to execute this Agreement on his or her behalf and to bind him or her with respect to the terms of this Agreement as if each of them had been a party hereto as an Author. The Author warrants that the use, reproduction, distribution, public or private performance or display, and/or modification of all or any portion of the Materials does not and will not violate, infringe and/or misappropriate the patent, trademark, intellectual property or other rights of any third party. The Author represents and warrants that it has and will continue to comply with all government, institutional and other regulations, including, without limitation all institutional, laboratory, hospital, ethical, human and animal treatment, privacy, and all other rules, regulations, laws, procedures or guidelines, applicable to the Materials, and that all research involving human and animal subjects has been approved by the Author's relevant institutional review board.

10. **JoVE Discretion.** If the Author requests the assistance of JoVE in producing the Video in the Author's facility, the Author shall ensure that the presence of JoVE employees, agents or independent contractors is in accordance with the relevant regulations of the Author's institution. If more than one author is listed at the beginning of this Agreement, JoVE may, in its sole discretion, elect not take any action with respect to the Article until such time as it has received complete, executed Article and Video License Agreements from each such author. JoVE reserves the right, in its absolute and sole discretion and without giving any reason therefore, to accept or decline any work submitted to JoVE. JoVE and its employees, agents and independent contractors shall have

ARTICLE AND VIDEO LICENSE AGREEMENT

full, unfettered access to the facilities of the Author or of the Author's institution as necessary to make the Video, whether actually published or not. JoVE has sole discretion as to the method of making and publishing the Materials, including, without limitation, to all decisions regarding editing, lighting, filming, timing of publication, if any, length, quality, content and the like.

11. **Indemnification.** The Author agrees to indemnify JoVE and/or its successors and assigns from and against any and all claims, costs, and expenses, including attorney's fees, arising out of any breach of any warranty or other representations contained herein. The Author further agrees to indemnify and hold harmless JoVE from and against any and all claims, costs, and expenses, including attorney's fees, resulting from the breach by the Author of any representation or warranty contained herein or from allegations or instances of violation of intellectual property rights, damage to the Author's or the Author's institution's facilities, fraud, libel, defamation, research, equipment, experiments, property damage, personal injury, violations of institutional, laboratory, hospital, ethical, human and animal treatment, privacy or other rules, regulations, laws, procedures or guidelines, liabilities and other losses or damages related in any way to the submission of work to JoVE, making of videos by JoVE, or publication in JoVE or elsewhere by JoVE. The Author shall be responsible for, and shall hold JoVE harmless from, damages caused by lack of sterilization, lack of cleanliness or by contamination due to the making of a video by JoVE its employees, agents or independent contractors. All sterilization, cleanliness or decontamination procedures shall be solely the responsibility of the Author and shall be undertaken at the Author's

expense. All indemnifications provided herein shall include JoVE's attorney's fees and costs related to said losses or damages. Such indemnification and holding harmless shall include such losses or damages incurred by, or in connection with, acts or omissions of JoVE, its employees, agents or independent contractors.

12. **Fees.** To cover the cost incurred for publication, JoVE must receive payment before production and publication the Materials. Payment is due in 21 days of invoice. Should the Materials not be published due to an editorial or production decision, these funds will be returned to the Author. Withdrawal by the Author of any submitted Materials after final peer review approval will result in a US\$1,200 fee to cover pre-production expenses incurred by JoVE. If payment is not received by the completion of filming, production and publication of the Materials will be suspended until payment is received.

13. **Transfer, Governing Law.** This Agreement may be assigned by JoVE and shall inure to the benefits of any of JoVE's successors and assignees. This Agreement shall be governed and construed by the internal laws of the Commonwealth of Massachusetts without giving effect to any conflict of law provision thereunder. This Agreement may be executed in counterparts, each of which shall be deemed an original, but all of which together shall be deemed to be one and the same agreement. A signed copy of this Agreement delivered by facsimile, e-mail or other means of electronic transmission shall be deemed to have the same legal effect as delivery of an original signed copy of this Agreement.

A signed copy of this document must be sent with all new submissions. Only one Agreement required per submission.

CORRESPONDING AUTHOR:

Name: Dr. Imke Atreya
Department: Department of Medicine 1
Institution: University Hospital of Erlangen
Article Title: Quantitative Imaging of Lung homing human Lymphocytes in a humanised...
Signature: [Signature] Date: 03.09.2010

Please submit a signed and dated copy of this license by one of the following three methods:

- 1) Upload a scanned copy of the document as a pdf on the JoVE submission site;
- 2) Fax the document to +1.866.381.2236;
- 3) Mail the document to JoVE / Attn: JoVE Editorial / 1 Alewife Center #200 / Cambridge, MA 02139

For questions, please email submissions@jove.com or call +1.617.945.9051

Point-by-Point-Reply

Editorial comments:

1. Please take this opportunity to thoroughly proofread the manuscript to ensure that there are no spelling or grammar issues.

We confirm that we carefully proofread our manuscript.

2. Please revise the protocol to contain only action items that direct the reader to do something (e.g., “Do this,” “Ensure that,” etc.). The actions should be described in the imperative tense in complete sentences wherever possible. Avoid usage of phrases such as “could be,” “should be,” and “would be” throughout the Protocol. Any text that cannot be written in the imperative tense may be added as a “Note.” Please include all safety procedures and use of hoods, etc. However, notes should be used sparingly and actions should be described in the imperative tense wherever possible.

The revised version of our protocol exclusively contains sentences written in the imperative tense. We avoided the use of terms like “could be”, “should be” and “would be”. Some few more notes were included into the protocol.

3. JoVE cannot publish manuscripts containing commercial language. This includes trademark symbols (™), registered symbols (®), and company names before an instrument or reagent. Please remove all commercial language from your manuscript and use generic terms instead. All commercial products should be sufficiently referenced in the Table of Materials and Reagents. You may use the generic term followed by “(see table of materials)” to draw the readers’ attention to specific commercial names. Examples of commercial sounding language in your manuscript are: eFluor, Imaris, Bitplane, etc.

The following terms have either been deleted or replaced by generic terms: MicroBeads, human (Miltenyi Biotec), eFluor 670, LaVision UltraMicroscope II Light Sheet Microscope, InspectorPro software, Imaris (Bitplane), Fiji.

4. 2.1.1-2.1.3: Please write the text in the imperative tense. Any text that cannot be written in the imperative tense may be added as a “Note.”

We optimized the text of the indicated paragraphs as recommended.

5. 4.5: Please specify the rotation speed.

We use a rotation speed of 31 rpm. This information has now been included into the protocol.

6. 5.2 and sub-steps: Please add more specific details (e.g. button clicks for software actions, numerical values for settings, etc.) to your protocol steps. For instance, what zoom factor is considered to be appropriate (5.1.6)? What sheet width is selected (5.1.7)? What are the start and end positions of the z-stack (5.1.10)?

More specific details including step-by-step bottom clicks in the software were now added to the section “5.2 Adjust settings at the light-sheet microscope to detect human cells in the context of the whole organ”. Additionally, numerical values for low and high magnification (6.3x and 32x, respectively), sheet NA (20 – 40 %) and the number of z-stack (300 - 800) are now indicated. However, ranges rather than exact values were chosen, since exact values critically depend on the specific tissue size and its positioning within the sample chamber and have to be determined for a specific experiment individually.

7. Please combine some of the shorter Protocol steps so that individual steps contain 2-3 actions and maximum of 4 sentences per step.

As suggested by the editors, we combined several of the shorter Protocol steps.

8. Please include single-line spaces between all paragraphs, headings, steps, etc.

The format was adopted accordingly.

9. After you have made all the recommended changes to your protocol (listed above), please highlight 2.75 pages or less of the Protocol (including headings and spacing) that identifies the essential steps of the protocol for the video, i.e., the steps that should be visualized to tell the most cohesive story of the Protocol.

We have highlighted selected steps that should be visualized (about 2.5 pages).

10. Please highlight complete sentences (not parts of sentences). Please ensure that the highlighted part of the step includes at least one action that is written in imperative tense. Please do not highlight any steps describing anesthetization and euthanasia.

All aspects have been considered.

11. Please include all relevant details that are required to perform the step in the highlighting. For example: If step 2.5 is highlighted for filming and the details of how to perform the step are given in steps 2.5.1 and 2.5.2, then the sub-steps where the details are provided must be highlighted.

We confirm that all relevant details have also been highlighted.

12. Figure 2: The labels on the scale bars are hard to read; please either enlarge or define the scale bars in the figure legend.

As suggested, we replaced and enlarged the scale bars.

13. References: Please do not abbreviate journal titles.

We now included full journal titles into References.

Comments provided by Reviewer #1:

Manuscript Summary:

Schulz-Kuhnt et al. describes a method of using light sheet microscopy to image lungs of immunodeficient animals with airway inflammation and added purified human T cells. This follows a model published by these authors describing a similar method imaging T cells in the gut.

Major Concerns:

While the introduction focuses on homing of T cells, it is not clear how this method can shed additional light on T cell homing to specific areas of the lung, especially as homing is dynamic and this study uses fixed tissue.

We thank the reviewer for thoroughly assessing our manuscript and providing helpful comments. The here described transfer of human T cells into recipient mice in combination with subsequently performed light-sheet fluorescence microscopy can indeed serve as a valuable tool to monitor lung homing of primary human immune cells, as the systemic circulation and organ distribution of transferred cells occurs within the living animal **prior to tissue fixation**. As described within the first NOTE of step 4 of our protocol, recipient mice were sacrificed only 3 hours after the transfer of human T cells, indicating that there is a period of 3 hours, in which *in vivo* lung homing is supposed to take place. Fixation of lung tissue is performed only in already sacrificed animals (see step 4.3 of our protocol) and allows to preserve the before *in vivo* achieved status of pulmonary immune cell infiltration.

Many studies have using live imaging of lung intravitaly to image immune cells in lung (see Lefrancais Nature 2017; Headley Nature 2016; Looney and Bhattacharya ARP 2014). These methods have also been used to image inflamed lung during airway inflammation (Hammad et al. Nat Med 2009; Bose et al. Plos One 2015), just to name a few. Additionally, new methods to image lung with light sheet microscopy have been published (Erturk et al. JOVE 2014; Mzinza et al. Cellular and Molecular Biology 2018). Note the publication in JOVE 2014. There is no reference to these other studies and how this method complements other methods of imaging lung.

The Introduction and Discussion of our manuscript have now been revised taking into account this comment. Indeed, the suggested discussion of the above mentioned publications relevantly improved the embedding of our manuscript into the current scientific context.

Besides light-sheet fluorescence microscopy, 2-Photon microscopy represents another very powerful tool for advanced lung imaging, which allows a detailed visualization of immune cells within the pulmonary microcirculation, but is clearly limited by a confined z-axis penetration. In contrast, the here applied light-sheet fluorescence microscopy of chemically cleared tissue shows a deep tissue penetration and thereby allows to quantify and describe

the intrapulmonary distribution of infiltrating immune cells within a complete pulmonary lobe. Accordingly, we now discuss that sequential performance of 2-photon microscopy and light-sheet fluorescence microscopy might represent a beneficial strategy to obtain, in the same experiment, a quantitative overview of the distribution and localization of human immune cells within the murine lung (light-sheet fluorescence microscopy) and, in addition, gain more detailed insights into cellular or microvascular processes (2-photon microscopy).

Compared to other studies, which already introduced light-sheet fluorescence microscopy as an advanced imaging tool in the field of pulmonology, our protocol shows the unique feature that it allows to characterize the lung accumulation and intrapulmonary distribution of primary human immune cells under experimentally defined inflammatory conditions. Thus, it combines the advantages of light-sheet fluorescence microscopy with the chance to directly analyze patient-derived immune cells in an *in vivo* scenario and thereby to potentially identify functional alterations imprinted by a particular disease or therapeutic regimens.

Light sheet microscopy depends on tissue clearing, and there are many methods that have different effects on tissue architecture. 4.7 does not specify what type of tissue clearing was used. There should be discussion of how tissues were cleared and how clear the tissue looked. An image of cleared lung would be helpful.

We have now specified the type of applied tissue clearing ("solvent-based clearing of the tissue using ethyl cinnamate") within the protocol and included a photo of successfully cleared lung tissue into Figure 1. Moreover, some important advantages of ethyl cinnamate-based protocols for tissue clearing have been described in the Discussion of the revised manuscript.

In the microscopy section it would be useful to be more quantitative. For example, 5.1.6 states "use low magnification", meaning 4X? 10X? More specificity would be helpful.

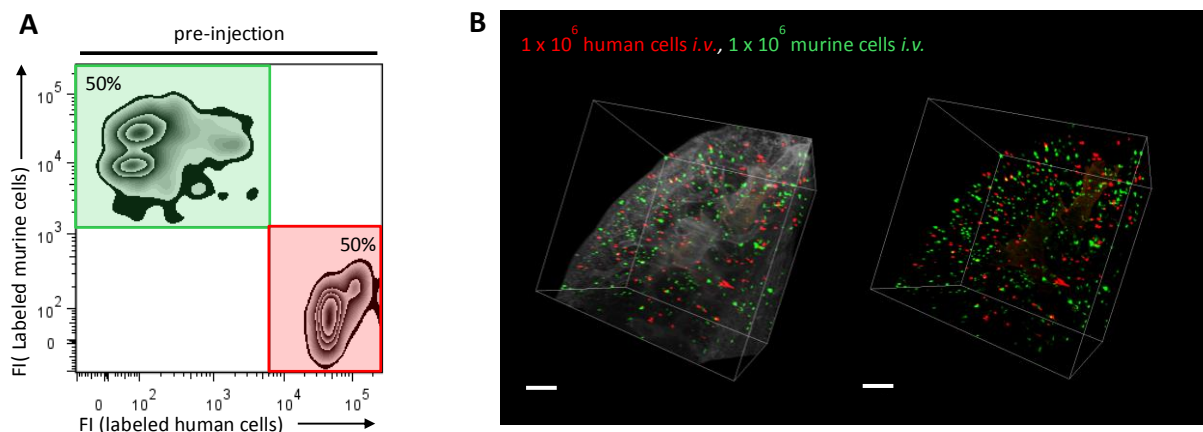
We thank the Reviewer for indicating this valid point. As suggested, we included more details in the microscopy section (see 5.2) including applied zoom factors (6.3x for low magnification and 32x for high magnification), sheet NA (20 - 40 %) and the number of z-stacks (300 - 800) that were usually acquired. We hope that these new details will improve reproducibility of our protocol.

Human T cells tend to be larger than mouse T cells, could this impact retention of T cells in small capillaries in lung? There is no quantitation or imaging of small vessels or which T cells remain in capillaries versus have extravasated. There should be some demonstration that these two populations can be distinguished.

It still remains challenging to image small pulmonary capillaries reliably via light-sheet fluorescence microscopy, even upon optimal clearing conditions. However, there exist alternative experimental strategies, which can be applied to confirm, characterize and/ or quantify extravasation of transferred human immune cells. These strategies (*e.g.* sequential

performance of 2-photon microscopy and light-sheet fluorescence microscopy) have now been discussed more extensively in the revised version of the manuscript.

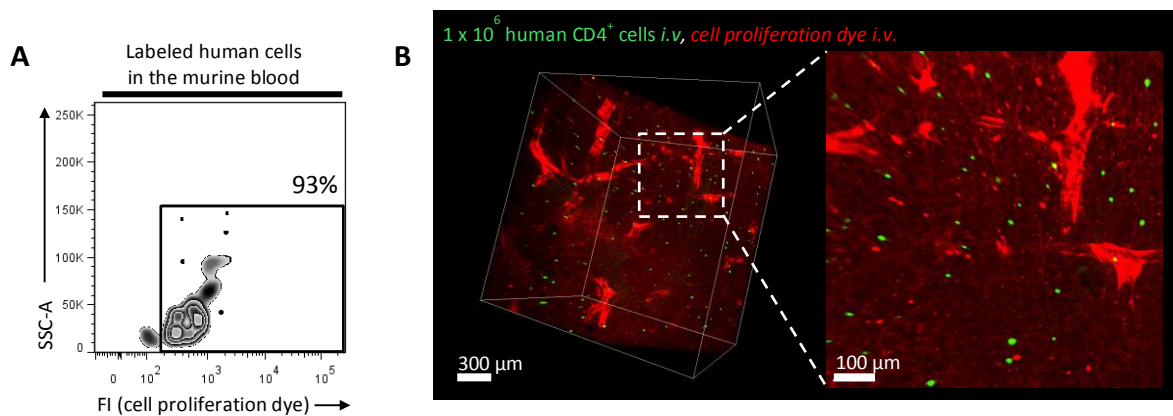
In order to experimentally address the Reviewers' concern that the larger size of human T cells and their potential mechanical retention within small lung capillaries might underlie the described accumulation of transferred human cells within the murine lung, we now performed a competitive transfer of human and murine immune cells into the same recipient animal. The acquired results are depicted below (**Point-by-Point-Reply Figure 1**) and clearly indicate that the intrapulmonary distribution pattern did not differ between transferred murine and human immune cells. For sure, the number of lung accumulated human cells was not higher than the number of murine cells, arguing against mechanical retention of human cells within murine lung capillaries.



Point-by-Point-Reply Figure 1: Competitive lung homing of human and murine immune cells. Mice with papain-induced airway inflammation were injected *i.v.* with a 50:50 mix of differently labeled human and murine cells. Human lymphoid cells derived from peripheral blood were stained with a cell proliferation dye with a peak emission of 670 nm. Murine spleen cells were stained with a cell proliferation dye with a peak emission of 580 nm. After 3 h, lung tissue was harvested and further prepared for light-sheet fluorescence microscopy. **(A)** Representative flow cytometric plot confirming equal amounts of differently labeled human (red) and murine lymphoid cells (green) within the prepared cell suspension prior to injection. **(B)** Representative 3D reconstructions of murine lungs imaged via light-sheet fluorescence microscopy. Scale bars represent 300 μm . Results are representative for $n = 2$. FI, fluorescence intensity.

In the Discussion of the revised manuscript, we now mention an interesting flow cytometric strategy for quantifying the extravasation of adoptively transferred immune cells within lung tissue (Galkina *et al.*; 2005). In this study, a single intravenous injection of a fluorescence-conjugated anti-CD8 antibody shortly before resection of the lung resulted in an exclusive and complete labeling of before transferred CD8⁺ T cells within the lung vascular compartment, while already extravasated CD8⁺ T cells within the lung interstitium remained unstained. Adapted to this experimental concept, we now performed a first pilot

experiment, in which we performed a single intravenous injection of a fluorescent cell proliferation dye shortly before resection of the lung. The used fluorophore differed from the one used for *ex vivo* labeling of human cells prior to transfer. Thus, intravascular human cells (double-positive for both fluorophores) could potentially be distinguished from extravasated human cells (single positive for the fluorophore, which was used for *ex vivo* labeling of human cells prior to transfer). As depicted in **Point-by-Point-Reply Figure 2A**, the vast majority (> 90 %) of human cells within the blood of recipient mice could indeed be characterized as double positive, thus confirming a successful labeling with the intravenously injected proliferation dye. Interestingly, subsequently performed light-sheet fluorescence microscopy of perfused and cleared lung tissue demonstrated that all retrieved human immune cells turned out to be negative for the intravenously injected proliferation dye (**Point-by-Point-Reply Figure 2B**), implicating that these cells had successfully left the pulmonary vasculature.



Point-by-Point-Reply Figure 2: Lung homing of *i.v.* injected human CD4⁺ cells in the described *in vivo* airway inflammation model. 1×10^6 labeled human CD4⁺ cells were injected *i.v.* into C57BL/6J mice with papain-induced airway inflammation. 3 h after the adoptive cell transfer, a cell proliferation dye with a different peak emission was injected *i.v.* to label intravascular cells. Afterwards, mice were sacrificed and murine blood and lung tissue were analyzed via flow cytometry and light-sheet fluorescence microscopy, respectively. **(A)** Representative flow cytometric plot gated on labeled human CD4⁺ cells in the murine blood. **(B)** Representative 3D reconstruction of murine lung tissue showing extravasated human CD4⁺ cells in green and intravascular cells stained with the *i.v.* injected dye in red. FI, fluorescence intensity.

Comments provided by Reviewer #2:

Manuscript Summary:

The manuscript described a technique to image lung infiltration of T cells. The similar lung fixation has been reported before. The light-sheet fluorescence microscopy looks like new to image the lung, but this microscopy has been described.

We would like to thank the reviewer for providing us with helpful comments. In the revised version of the manuscript, it has now been clearly stated that light-sheet fluorescence microscopy has already been established successfully as an important tool for advanced lung imaging. Moreover, we now refer to already published protocols describing *in situ* lung fixation.

Major Concerns:

The title of manuscript is confusing and not correct. In the study, the authors used C57 mice rather humanized mice. Secondly, there is not quantitative analysis of images, so it is confusing to use "Quantitative imaging" term.

We have changed the title of our manuscript, taking into account the Reviewers' concerns.

Comments provided by Reviewer #3:

Manuscript Summary:

This is a very interesting study where the authors were able to demonstrate *in vivo* monitoring of human lymphocytes infiltration into the lungs with induced inflammation in a mouse model.

We thank the Reviewer for this positive feedback.

Major Concerns:

none

Minor Concerns:

1. minor editing of the manuscript is required.

We now prepared a carefully revised version of our manuscript, which includes a slightly extended Discussion, additional subfigures and some clarifications regarding the described experimental procedure. Overall, we hope that we were able to further improve the quality of our manuscript.

2. not sure why some parts of the manuscript was highlighted with yellow color. Please remove the highlight during revision.

Based on the JoVE guidelines for manuscript preparation, we highlighted parts of the Protocol in order to indicate the essential steps of the protocol, which should later be visualized in the video. As this highlight is necessary for the further editorial processing of our manuscript, we did not remove it.